



Published in final edited form as:

Neuron. 2008 May 22; 58(4): 507–518.

Nervous wreck interacts with Thickveins and the endocytic machinery to attenuate retrograde BMP signaling during synaptic growth

Kate M. O'Connor-Giles^{*}, Ling Ling Ho, and Barry Ganetzky

Laboratory of Genetics, University of Wisconsin-Madison, Madison, WI 53706

Summary

Regulation of synaptic growth is fundamental to the formation and plasticity of neural circuits. Here we demonstrate that Nervous wreck (Nwk), a negative regulator of synaptic growth at *Drosophila* NMJs, interacts functionally and physically with components of the endocytic machinery, including dynamin and Dap160/Intersectin, and negatively regulates retrograde BMP growth signaling through a direct interaction with BMP receptor, Thickveins. Synaptic overgrowth in *nwk* is sensitive to BMP signaling levels and loss of Nwk facilitates BMP-induced overgrowth. Conversely, Nwk overexpression suppresses BMP-induced synaptic overgrowth. We observe analogous genetic interactions between *dap160* and the BMP pathway, confirming that endocytosis regulates BMP signaling at NMJs. Finally, we demonstrate a correlation between synaptic growth and pMAD levels, and show that Nwk regulates these levels. We propose that Nwk functions at the interface of endocytosis and BMP signaling to ensure proper synaptic growth by negatively regulating Tkv to set limits on this positive growth signal.

Introduction

The formation and plasticity of neural circuits depends on the proper establishment and remodeling of synapses in response to environment and experience. The *Drosophila* larval neuromuscular junction (NMJ) has become a powerful model system for dissecting the molecular mechanisms that regulate synaptic growth (Collins and DiAntonio, 2007). NMJs are dynamic structures that coordinate their size and strength with muscle growth and undergo changes in morphology and physiology in response to environmental stimuli and altered levels of activity (Budnik et al., 1990; Sigris et al., 2003; Sigris et al., 2002).

It is well established that neurons and muscles are in communication to coordinate the development and refinement of pre- and postsynaptic terminals (Haghighi et al., 2003; Marrus and DiAntonio, 2004; Nakayama et al., 2006; Packard et al., 2002; Pielage et al., 2006; Saitoe et al., 2001). Identification of the factors that mediate trans-synaptic coordination of NMJ development has been a key objective for understanding synaptic growth and plasticity. Several recent studies have identified the bone morphogenic protein (BMP) signaling pathway as a critical retrograde (muscle to neuron) growth signal that regulates NMJ development (Aberle et al., 2002; Marques et al., 2002; McCabe et al., 2004; McCabe et al., 2003; Rawson et al., 2003; Sweeney and Davis, 2002). BMPs are members of the transforming growth factor- β

*Correspondence: oconnorgiles@wisc.edu.

Publisher's Disclaimer: This is a PDF file of an unedited manuscript that has been accepted for publication. As a service to our customers we are providing this early version of the manuscript. The manuscript will undergo copyediting, typesetting, and review of the resulting proof before it is published in its final citable form. Please note that during the production process errors may be discovered which could affect the content, and all legal disclaimers that apply to the journal pertain.

(TGF- β) superfamily of signaling proteins (Miyazono et al., 2001). At *Drosophila* NMJs, the BMP Glass bottom boat (Gbb) is released, presumably by muscles, to activate BMP receptors, Wishful thinking (Wit), Thickveins (Tkv) and Saxophone (Sax) at presynaptic terminals. These receptors represent two classes of transmembrane serine/threonine kinases. Upon ligand binding, Wit, a type II receptor, forms a complex with the type I receptors Tkv and Sax. In turn, phosphorylation of Tkv and Sax by Wit induces them to phosphorylate the receptor-regulated R-Smad Mothers against Dpp (Mad). Mad is a cytoplasmic signal transduction effector that, when phosphorylated, binds the co-Smad Medea (Med) and translocates to the nucleus where the complex activates or represses transcription of target genes (Keshishian and Kim, 2004). Mutations in *gbb*, *wit*, *tkv*, *sax*, *mad* and *medea* all result in pronounced NMJ undergrowth (Aberle et al., 2002; Marques et al., 2002; McCabe et al., 2004; McCabe et al., 2003; Rawson et al., 2003).

An important open question is whether BMP signaling is required simply as a permissive switch to initiate synaptic growth or instead is instructive, modulating synaptic growth in a graded fashion in proportion to signal levels. In the latter case, BMP signaling is itself likely to be subject to positive and negative regulation to fine tune signaling levels in response to external and internal cues. Such regulation could occur at a number of levels including presynaptic regulation of available receptors or trafficking of activated receptor signaling complexes and postsynaptic regulation of Gbb release.

nervous wreck (nwk) was identified as a neuron-specific negative regulator of NMJ growth in a secondary screen of temperature-sensitive paralytic mutants for aberrant synaptic morphology (Coyle et al., 2004). Nwk is the *Drosophila* representative of a family of proteins, conserved from yeast to humans. A human family member has been identified as the affected gene in a heritable form of mental retardation, highlighting a conserved role for Nwk and Nwk-related proteins in neural development. Nwk-family proteins share a distinctive domain architecture including a newly defined F-BAR domain (Itoh et al., 2005), two SH3 domains (or in some cases one SH3 and one RhoGAP domain), and a C-terminal proline-rich domain (PRD) with numerous PxxP SH3-binding sites. F-BAR domains induce membrane invagination and have been identified in proteins associated with both actin regulation and endocytosis. SH3 domains mediate protein-protein interactions and are commonly found in adaptor proteins in signal transduction pathways. The activity of the Wiscott-Aldrich Syndrome Protein, Wasp, which promotes F-actin assembly by activating the ARP2/3 (actin-related protein) complex, is regulated in part by interacting directly with SH3-domain containing proteins transmitting upstream growth signals (Takenawa and Suetsugu, 2007). Nwk was found to bind Wasp via its first SH3 domain (Coyle et al., 2004). Furthermore, mutations in *wasp* result in synaptic overgrowth similar to that of *nwk* and enhance *nwk* mutants in a dose-dependent manner suggesting that Nwk and Wasp are components of a common pathway regulating NMJ growth. These data suggest Nwk may function by linking growth cues to reorganization of the actin cytoskeleton during synaptic growth.

A number of endocytic proteins, among them dynamin, Dap160/Intersectin, Endophilin, Synaptojanin, Rab11 and Spinster (Spin) have also been identified as negative regulators of NMJ growth (Dickman et al., 2006; Khodosh et al., 2006; Koh et al., 2004; Marie et al., 2004; Sweeney and Davis, 2002). Mutations in the majority of these genes share with *nwk* the specific morphological defect of supernumerary or satellite bouton formation (Dickman et al., 2006). *shibire (shi, Drosophila* dynamin) encodes a GTPase that is required for the scission of endocytic vesicles from the plasma membrane. Dap160, originally identified as a binding partner of dynamin, is a scaffolding protein required for the stable formation of a complex of endocytic proteins at presynaptic terminals. In addition to the defined role of these proteins in synaptic vesicle endocytosis at the NMJ, disrupted endocytosis and trafficking of growth signaling receptors may underlie their synaptic overgrowth phenotypes. In fact, *spin* encodes

a late endosomal/lysosomal protein proposed to function, at least in part, in the downregulation of BMP signaling at synapses (Sweeney and Davis, 2002). Recent evidence from a variety of experimental systems has shown that endocytosis is dependent on the precise spatial and temporal regulation of actin assembly (Itoh and De Camilli, 2006; Kim and Chang, 2006; Smythe and Ayscough, 2006). Further, it is becoming increasingly apparent that endocytosis is a key mechanism for the integration and regulation of cell signaling pathways (Conner and Schmid, 2003; Di Fiore and De Camilli, 2001). Together, these findings raise the possibility that *nwk* mutants disrupt an actin-dependent endocytic mechanism required for the negative regulation of a synaptic growth signal.

In support of this idea, we have found that Nwk interacts functionally and physically with components of both the endocytic machinery and the BMP signaling pathway. Synaptic overgrowth in *nwk* is sensitive to the dosage of presynaptic BMP receptors and loss of Nwk facilitates BMP-induced synaptic overgrowth. We also found that ectopic BMP signaling results in varying levels of synaptic overgrowth depending on the dose of activated receptor, supporting an instructive role for BMP signaling in synaptic growth, and we demonstrate that overexpression of Nwk suppresses this phenotype. Consistent with a role for Nwk in the regulation of BMP signaling levels, we observe a direct physical interaction between Nwk and Tkv. Finally, we demonstrate a correlation between synaptic growth and pMAD levels, and show that these levels are regulated by Nwk. Based on these results, we propose that Nwk functions at the intersection of actin-dependent endocytosis and BMP signaling to constrain synaptic growth through the endocytic regulation of the presynaptic BMP receptor Tkv.

Results

Synaptic overgrowth in *nwk* is dominantly enhanced by endocytic mutations

Previous work suggests Nwk negatively regulates synaptic growth at least in part through effects on actin assembly via its direct interactions with Wasp (Coyle et al., 2004). Although actin is involved in a number of mechanisms required for synaptic growth including cell adhesion and process extension, a number of observations led us to hypothesize that Nwk may function at the convergence of actin assembly and endocytosis. First, *nwk* NMJs display a distinctive phenotype of satellite bouton formation and hyperbudding, in which a given bouton sprouts three or more daughter boutons. A similar phenotype has recently been observed in a number of endocytic mutants, including *endo* and *dap160*, suggesting a link between the formation of satellite boutons and defects in endocytosis (Dickman et al., 2006; Khodosh et al., 2006; Koh et al., 2004; Marie et al., 2004). Second, Nwk colocalizes with endocytic proteins at the periaxial zones of boutons, including sites of active endocytosis as indicated by dynamin-positive “hot spots” (Coyle et al., 2004; Estes et al., 1996; Roos and Kelly, 1999). Third, Nwk levels are reduced in the absence of endocytic scaffolding protein Dap160 (Koh et al., 2004). Fourth, a large body of recent work has revealed that endocytosis is accompanied by spatially and temporally regulated bursts of actin assembly. Moreover, there is extensive overlap between endocytic proteins and regulators of actin assembly, reflecting the importance of actin-dependent steps in the internalization and trafficking of endocytic vesicles (Itoh and De Camilli, 2006; Kim and Chang, 2006; Smythe and Ayscough, 2006). Finally, recent work in vertebrates has identified a novel domain, named F-BAR, that is able to induce plasma membrane invagination (Itoh et al., 2005). An F-BAR domain is present in Nwk and its vertebrate orthologs.

To explore the possibility that Nwk functions in a common pathway with endocytic proteins during synaptic growth, we assayed genetic interactions between *nwk* and mutations in a number of known endocytic genes, including *dap160*, *endophilin (endo)* and *shi*. For each of these we observe significant dominant enhancement of both bouton number and satellite bouton formation at all *nwk* NMJs (Figure 1). To quantify this phenotypic enhancement, we focused

on NMJ 4, a simple, stereotypic synapse formed by motor neuron 4-1b on the face of muscle 4 (Hoang and Chiba, 2001). Satellite boutons were defined in accordance with Dickman et al. (2006) as extensions of 5 or fewer boutons emanating from the main branch of the nerve terminal (See arrows in Figure 1B). Mutations in *nwk* result in a 1.5-fold increase in bouton number and a 3-fold increase in the formation of satellite boutons (Figures 1A–B, I–J). Loss of one copy of *endo* in a *nwk* mutant background increases bouton number 1.5-fold and causes a 3.4-fold increase in satellite bouton formation, but has limited effect in a wild-type background (Figures 1C–D, I–J). Similarly, heterozygous mutations in *dap160* have no effect on wild-type synapses but cause a 2.5-fold increase in satellite bouton formation and a 1.2-fold increase in bouton number at *nwk* synapses (Figures 1E–F, I–J). It was previously shown that *shi^{ts1}* mutant larvae raised at the semi-restrictive temperature of 25°C exhibit a 5-fold increase in satellite boutons compared with wild type (Dickman et al., 2006). At this temperature, we did not observe a significant increase in satellite bouton formation in *shi* heterozygotes alone (Figures 1G and J) but did see significant dominant enhancement of the *nwk* phenotype (Figures 1H–J). These results place Nwk in a common pathway with endocytic proteins at presynaptic terminals.

Nwk physically interacts with the endocytic machinery

Given the strong phenotypic interactions between *nwk* and mutations affecting known endocytic proteins as well as the colocalization of these proteins at presynaptic periaxonal zones and endocytic hot spots, we investigated whether Nwk physically associates with the endocytic machinery by GST-pulldown and yeast two-hybrid experiments. Both Dap160 and dynamin GST-fusion proteins precipitate Nwk from fly lysates with high efficiency. Furthermore, pulldown experiments with GST fusions of specific Dap160 and dynamin domains demonstrate that it is the SH3 domains of Dap160 and the proline-rich domain (PRD) of dynamin that bind Nwk (Figures 2A and B).

To determine if the interactions of Nwk with Dap160 and dynamin are direct, we performed yeast two-hybrid experiments. Growth of yeast cells co-transformed with Nwk and either Dap160 or dynamin constructs and grown on multiple selective media reveals direct binding between Nwk and both endocytic proteins (Figure 2C). Finally, we investigated the potential for Nwk, dynamin and Dap160 to interact as a complex. Because Nwk binds dynamin through its SH3 domains and binds Dap160 through its PRD, it has the capacity to bind both proteins simultaneously. On the other hand, both Nwk and dynamin bind the SH3 domains of Dap160 and might compete for the same binding site. The interaction between Dap160 and dynamin is mediated exclusively by the SH3a and b domains of Dap160 (Roos and Kelly, 1998). We performed pulldown experiments with GST constructs containing either the SH3a and b or the SH3c and d domains of Dap160. The SH3c and d domains of Dap160 precipitate Nwk with high affinity, while the SH3a and b domains do not (Figure 2D). Thus, Dap160 has the capacity to form a multi-protein complex containing Nwk and dynamin. These findings are consistent with data from *Drosophila* and vertebrates indicating that Dap160/Intersectin is a scaffolding protein responsible for coordinating the activities of a number of proteins that bind sequentially as endocytosis progresses (Hussain et al., 2001; Koh et al., 2004; Marie et al., 2004; Roos and Kelly, 1998; Zamanian and Kelly, 2003).

Synaptic overgrowth in *nwk* depends on the level of retrograde BMP signaling

Nwk's role as a negative regulator of synaptic growth together with the phenotypic, genetic and biochemical evidence indicating a functional association between Nwk and the endocytic machinery suggested Nwk might be required for downregulation of a positive growth signal at the NMJ. A number of recent studies demonstrate that the BMP signaling pathway constitutes the primary positive retrograde growth signal at developing NMJs (Aberle et al., 2002; Marques et al., 2002; McCabe et al., 2004; McCabe et al., 2003; Rawson et al., 2003; Sweeney and

Davis, 2002), so we examined genetic interactions between *nwk* and BMP pathway components.

The BMP pathway is required for synaptic overgrowth in *nwk* mutants as loss of *wit* fully suppresses the synaptic overgrowth observed in *nwk* mutants (Figures 3A–H, K). At NMJ 4, wild-type synapses have an average of 21 boutons (Figures 3B and K), compared with 30 in *nwk* (Figures 3D and 3K). Conversely, *wit* mutants are severely undergrown, with an average of 7.9 boutons per NMJ 4 (Figures 3F and K). In *nwk wit* double mutants, the average number of boutons at NMJ 4 is essentially the same as in *wit* single mutants (Figures 3H and K). Thus, synaptic overgrowth in *nwk* requires BMP signaling.

Furthermore, we have found that the *nwk* phenotype depends on wild-type levels of Wit, supporting the idea of a direct link between the level of BMP signaling and synaptic overgrowth in *nwk*. Loss of one copy of *wit*, which has no effect in a wild-type background, significantly suppresses synaptic overgrowth in *nwk* mutants (Figures 3J and K). We observe similar dosage-sensitive interactions between *nwk* and all other components of the BMP signaling pathway analyzed, including *gbb*, *tkv*, *med* and *mad* (data not shown). These findings are consistent with a model in which Nwk restrains synaptic growth via the endocytic downregulation of BMP signaling.

Nwk constrains BMP-induced synaptic overgrowth

Overexpression of a constitutively active Tkv receptor (Tkv^{ACT}) causes striking gain-of-function phenotypes in a number of tissues, notably the developing wing (Hoodless et al., 1996). At the NMJ, neuronal expression of Tkv^{ACT} does not affect synaptic growth (McCabe et al., 2004) (Figures 4A, C and E). One possibility is that BMP signaling is constrained at the NMJ by mechanisms that set upper limits on the pathway. If Nwk were acting to set a limit on BMP signaling, we would expect its removal to permit Tkv^{ACT} -induced synaptic overgrowth. In analogous experiments, expression of Tkv^{ACT} in *highwire* (*hiw*) mutants resulted in an increase in bouton formation beyond that observed in the absence of *Hiw* alone (McCabe et al., 2004). We found that neuronal expression of Tkv^{ACT} in *nwk* mutants does not cause a significant increase in bouton number compared with *nwk* alone (data not shown). However, Tkv^{ACT} expression in a *nwk* background results in a 1.7-fold increase in satellite bouton formation over that observed in *nwk* alone (Figures 4B–E). These results indicate that indeed Nwk does play a role in downregulating BMP signaling at the NMJ and that this regulation is particularly important for controlling the emergence of satellite boutons.

BMP-induced synaptic overgrowth is suppressed by overexpression of Nwk

If the level of BMP signaling at the NMJ plays an instructive role in determining the extent of synaptic growth, further manipulation of Tkv^{ACT} expression might result in synaptic overgrowth. In fact, we found that neuronal expression of two copies of UAS_{tkv}^{ACT} via *CI55GAL4* results in a 2-fold increase in bouton number and 4-fold increase in satellite bouton formation (Figures 5A–D, K–L). We do not observe overgrowth in the absence of *GAL4* indicating that the phenotype is dependent on overexpression of tkv^{ACT} and not the result of a second-site mutation (Figures 5K and L). Consistent with previous studies in the embryonic CNS, we also found that co-overexpression of one copy each of Tkv^{ACT} and Sax^{ACT} results in synaptic overgrowth (Allan et al., 2003)(data not shown). Hence, increased levels of BMP signaling cause corresponding increases in synaptic growth in general and the formation of satellite boutons, in particular. The similarity of this phenotype to that associated with defects in endocytosis is consistent with the idea that a common mechanism is disrupted in both cases.

If Nwk acts to downregulate BMP signaling, then simultaneous overexpression of wild-type *nwk* in neurons should counteract the effect of two doses of UAS_{tkv}^{ACT} . We found that

coexpression of a single copy of *UASnwk* suppresses the increase in both bouton number and satellite boutons (Figures 5E–F, K–L), while *Nwk* expression in a wild-type background does not affect synaptic growth (Figures 5K and L). The suppression of synaptic overgrowth by *UASnwk* is not simply an indirect consequence of the dilution of *GAL4* by the presence of a third UAS element because coexpression of *UASmyrRFP* does not suppress the overgrowth phenotypes (Figures 5K and L). These results demonstrate the ability of *Nwk* to limit BMP signaling levels at NMJs.

Synaptic overgrowth in *Dad* mutants is suppressed by overexpression of *Nwk*

The NMJ phenotypes of larvae ectopically expressing *Tkv^{ACT}* indicates that sufficiently high levels of BMP signaling cause synaptic overgrowth. To investigate this further, we examined NMJ morphology in *Dad* mutants, in which loss of the inhibitory Smad should result in a substantial increase in endogenous BMP signaling (Sweeney and Davis, 2002). We observed significant synaptic overgrowth in all *Dad* mutant combinations examined. For example, bouton number in *Dad^{J1e4}* mutants is 1.8 fold greater than wild type and satellite bouton formation is increased 4.8-fold (Figures 5G–H, K–L). At *Dad^{J1e4}/Dad²⁷¹⁻⁶⁸* NMJs, bouton number is doubled with a 4.8-fold increase in satellite boutons (Figures 5K–L). We observed similar levels of overgrowth in hemizygous backgrounds, confirming a role for *Dad* in the negative regulation of BMP-dependent synaptic growth at larval NMJs.

If *Nwk* downregulates BMP signaling then increased levels of *Nwk* should also mitigate the phenotypic effects of loss of negative regulation of endogenous BMP signaling by *Dad*. To test this, we expressed *Nwk* pan-neuronally in *Dad* mutants, and found that *Nwk* overexpression does, in fact, suppress *Dad*. Specifically, we found that bouton number is significantly reduced by *Nwk* expression in a *Dad* mutant, as is the incidence of satellite boutons (Figures 5I–L). These data provide further evidence that *Nwk* normally acts to limit BMP signaling at NMJs.

dap160 interacts with BMP signaling pathway components

Our genetic and biochemical data suggest that synaptic overgrowth and satellite bouton formation in *nwk* and other endocytic mutants may occur through a common mechanism, specifically the failure to appropriately downregulate BMP signaling. This model predicts that satellite bouton formation and synaptic overgrowth in other endocytic mutants are also sensitive to BMP signaling levels. We directly tested this by investigating genetic interactions between *dap160* and components of the BMP signaling pathway. First, we analyzed *dap160; wit* double mutants and the effect of reducing *wit* dosage on synaptic overgrowth at *dap160* NMJs. *dap160; wit* double mutants exhibit synaptic undergrowth similar to that observed in *wit* mutants, and loss of one copy of *wit* suppresses synaptic overgrowth at *dap160* synapses (Figures 6A–C, G). These results demonstrate that synaptic overgrowth in *dap160* mutants, as in *nwk*, is dependent upon and sensitive to the dosage of BMP signaling. Next, we tested whether Dap160 also constrains BMP signaling levels by assaying the effect of removing *dap160* on the ability of one copy of *Tkv^{ACT}* to induce synaptic overgrowth. We found that loss of one copy of *dap160* is sufficient to enable one copy of *Tkv^{ACT}* to induced synaptic overgrowth (Figures 6D, G–H). Finally, we investigated the ability of Dap160 overexpression to suppress BMP-induced synaptic overgrowth. At NMJs expressing two copies of *Tkv^{ACT}* or mutant for *Dad*, we found that neuronal overexpression of Dap160 suppressed both total and satellite bouton number (Figures 6E–I). These results demonstrate that Dap160 regulates BMP signaling and provide strong support for our model that BMP-dependent growth at presynaptic terminals is attenuated via endocytic regulation by proteins such as *Nwk*, Dap160, and their interacting partners.

Nwk physically associates with the BMP receptor Tkv

The model that Nwk functions with the presynaptic endocytic machinery to downregulate retrograde BMP growth signaling implies Nwk is a component of an endocytic mechanism that acts to limit the abundance or signaling capacity of membrane-associated BMP receptors. Thus, Nwk may physically interact with one or more of the BMP receptors, providing a link between BMP receptors and the endocytic machinery, to regulate their trafficking or degradation via receptor-mediated endocytosis. Consistent with the possibility of physical association *in vivo*, we found that Nwk and neuronally expressed Tkv-GFP both localize to presynaptic periaxial zones where they colocalize to puncta consistent with endocytic vesicles (Figures 7A and 7B) (Hsiung et al., 2005). Moreover, the intracellular domain of Tkv (Tkv-IC) expressed as a GST-fusion construct efficiently precipitates Nwk from fly lysates (Figure 7C). We also conducted the reciprocal pulldown experiment and found that GST-Nwk precipitates full-length Tkv from fly lysates (Figure 7D). Thus, either full-length Tkv or its intracellular domain alone can physically associate with Nwk. The presence of multiple PxxP SH3-binding domains in Tkv-IC, raised the possibility of a direct interaction, and yeast two-hybrid experiments confirm that the association between Nwk and Tkv-IC is direct (Figure 7E). Together, these findings support the mechanistic interpretation that Nwk attenuates BMP signaling via endocytic regulation of Tkv.

Presynaptic pMAD levels correlate with synaptic growth and are regulated by Nwk

Activation of BMP receptors leads to the phosphorylation of Mad. Thus, pMAD levels serve as a molecular read out of BMP signaling levels at presynaptic terminals. Our model that Nwk negatively regulates BMP signaling at presynaptic terminals predicts an increase in pMAD levels in *nwk* mutants. To test this, we quantified pMAD levels at wild-type and *nwk* synapses and found that pMAD levels are substantially higher (3.3-fold) in *nwk* mutants (Figures 8A–B, I). A recent study posited an anterograde BMP signal at the NMJ based on the observation of postsynaptically localized pMAD (Dudu et al., 2006). To confirm that the ectopic pMAD we observe is presynaptic, we co-labeled *nwk* synapses with pMAD and pre- and postsynaptic markers, including Bruchpilot (Brp), which labels presynaptic active zones, and Discs large (Dlg), which labels postsynaptic membrane. We found significant overlap between pMAD and Brp, but essentially no overlap between pMAD and Dlg at *nwk* NMJs, indicating that the ectopic pMAD is primarily or entirely presynaptic (Figures 8B and C).

The model that Nwk is functioning with the endocytic machinery to regulate BMP signaling, suggests that mutations in other endocytic proteins will also result in increased pMAD levels. In fact, a recent study of the *Drosophila* spastic paraplegias protein Spichthyin (Spict), an early endosome-associated protein that negatively regulates synaptic growth, reported a more than 3-fold increase in presynaptic pMAD levels at *spict* NMJs (Wang et al., 2007). We investigated pMAD levels in *dap160*, *shi*, and *endo* mutants and observed increases in all three backgrounds, with the most significant increase (5.7-fold) found in *endo* mutants (Figures 8D and I). Our model further predicts a correlation between BMP-induced synaptic growth and pMAD levels and the modulation of these levels by Nwk. A previous study found an approximately 50% increase in nuclear pMAD levels in larvae expressing Tkv^{ACT} (Collins et al., 2006). We observe a similar Tkv^{ACT}-induced increase both in motor neuron nuclei and at the NMJ, where pMAD levels are 42% higher than wild type (Figures 8E and I). Consistent with our model, we observe a much larger (6.4-fold) increase in presynaptic pMAD when two copies of Tkv^{ACT} are expressed (Figures 8G and I). Significantly, we also found that these levels are regulated by Nwk. Removing Nwk from larvae expressing one copy of Tkv^{ACT}, which we have found causes a further increase in synaptic growth, results in a 7.8-fold increase in pMAD levels over wild type and a 2.3-fold increase over *nwk* levels (Figures 8F and I). Conversely, overexpression of Nwk in larvae expressing two copies of Tkv^{ACT} reduces pMAD levels 3.3-fold, which is consistent with Nwk's ability to suppress BMP-induced synaptic overgrowth

(Figures 8H and I). Finally, we observe a correspondence between pMAD levels and satellite bouton formation (Figure 8I). These data demonstrate a clear relationship between synapse morphology and BMP signaling levels, and confirm that Nwk regulates these levels.

Discussion

This work presents a model for the endocytic regulation of retrograde BMP signaling at synapses, integrating the roles of known positive and negative regulators of synaptic growth into a common molecular pathway. Specifically, our findings indicate that Nwk negatively regulates Tkv trafficking through an endocytic mechanism to limit retrograde BMP signaling, thereby constraining synaptic growth.

A role for Nwk in receptor endocytosis

Nwk interacts functionally and physically with a number of known endocytic proteins, notably dynamin and Dap160. FM1-43 uptake experiments showed that Nwk does not function in an internalization step of synaptic vesicle endocytosis (Coyle et al., 2004), suggesting Nwk affects a later step in endocytic trafficking. In agreement, we observe colocalization between Nwk and the recycling endosome-associated Rab GTPase Rab11, but not between Nwk and Rab proteins associated with either early or late endosomes (unpublished results). Consistent with this observation, Khodosh et al. (2006) found that hypomorphic mutations in *Drosophila rab11* result in a synaptic overgrowth phenotype that very closely resembles *nwk*.

Importantly, Nwk, Dap160 and dynamin are all linked to regulation of actin assembly (Coyle et al., 2004; Engqvist-Goldstein and Drubin, 2003; Hussain et al., 2001). Recent experiments demonstrate that dynamin-mediated vesicle fission requires actin polymerization. For example, Itoh et al. (2005) found that inhibiting actin polymerization blocks fission. Nwk likely facilitates a critical interaction between the endocytic machinery and actin polymerization at NMJs since it directly binds both dynamin and Wasp. Nwk also contains an F-BAR domain, which promotes membrane invagination (Itoh et al., 2005). These domains are found almost exclusively in adaptor proteins that associate both with actin regulators and the endocytic machinery, highlighting the important links between these cellular processes.

The critical role of endocytic accessory proteins in linking the core endocytic machinery to cell signaling molecules is becoming increasingly clear (Conner and Schmid, 2003; Di Fiore and De Camilli, 2001). In addition to attenuating signaling by targeting receptors for degradation, endocytic adaptor proteins play key roles in spatial and temporal regulation of signal transduction from ligand-activated receptors. Recent work in other systems also suggests a critical role for endocytic trafficking during TGF- β /BMP signal transduction. For example, Smad phosphorylation and nuclear translocation in vertebrates depend on localization of the endosomal protein, Smad anchor for receptor activation (SARA), and activated type I and II receptors to EEA1-positive endosomal compartments (Hayes et al., 2002). Similarly, in the *Drosophila* wing, targeting of Sara, Tkv and the ligand Decapentaplegic (Dpp) to early endosomes is required for productive signaling (Bokel et al., 2006). Nwk is ideally situated to bridge endocytosis and growth signal regulation at presynaptic terminals because of its links to actin assembly and endocytosis as well as its capacity for binding a number of proteins – including Tkv – through its multiple protein-protein interaction domains.

Endocytosis, growth signaling and satellite bouton formation

Many cellular processes have been implicated in negative regulation of synaptic growth, including cell adhesion, ubiquitin-dependent protein degradation, actin dynamics and endocytosis, while studies in *Drosophila* and vertebrates demonstrate a direct correlation between morphological growth and physiological plasticity (Collins and DiAntonio, 2007;

Dillon and Goda, 2005). Loss of endocytic proteins results in the specific phenotype of excessive satellite bouton formation (Dickman et al., 2006), as do mutations in actin-associated proteins, including Nwk, Wasp and components of the Scar complex (Coyle et al., 2004; Koh et al., 2004; Marie et al., 2004; Schenck et al., 2004). These observations suggest that satellite bouton formation is a specific result of impairment of an actin-dependent step in endocytosis. Dickman et al. (2006) suggested the possible misregulation of a signaling pathway responsible for bouton growth and morphology in endocytic mutants and, because satellite bouton formation had not been linked with any known pathway, postulated existence of either an unidentified positive growth signal downregulated by endocytosis or an endocytosis-dependent negative growth signal. Here we show that BMP signaling regulates satellite bouton formation. Increasing levels of BMP signaling, either by expressing *UAS^{ACT}tkv* or by reducing endogenous negative regulation of the pathway, generates a significant increase in satellite bouton formation. Further, overexpression of Nwk or Dap160 suppresses BMP-induced overgrowth, including satellite bouton formation. Together, these results indicate that impaired endocytic regulation of retrograde BMP signaling results in generation of satellite boutons at NMJs. In the case of endocytic and *Dad* mutants, downregulation of endogenous BMP signaling is impaired, while in *Tkv^{ACT}*-expressing larvae, ectopic BMP signaling apparently overwhelms the usual mechanisms of negative regulation.

A model of Nwk-dependent endocytic regulation of BMP signaling

Although BMP signaling is required for NMJ growth, it has remained unclear whether the signal acts merely as a switch to initiate or permit growth or instead plays a more instructive role in regulating and coordinating synaptic growth (Aberle et al., 2002; Marques et al., 2002; McCabe et al., 2004; McCabe et al., 2003; Rawson et al., 2003; Sweeney and Davis, 2002). Here, we demonstrate a direct relationship between levels of BMP signaling and extent of synaptic growth. Neuronal expression of a single copy of *Tkv^{ACT}* results in modest increase in pMAD and no significant increase in synaptic growth, whereas expression of two copies induces a dramatic increase in pMAD levels and extensive synaptic overgrowth – both of which are suppressed by overexpression of Nwk. Further, in agreement with Sweeney and Davis (2002), we find that mutations in the endogenous negative regulator *Dad* also cause increased synaptic growth (Sweeney and Davis, 2002). These data indicate that the level of BMP signaling has an instructive role in governing synaptic size and complexity, and reveal the importance of interactions between positive and negative regulators that modulate the growth signal in response to internal and external cues.

Our results demonstrate that endocytosis is an important regulatory mechanism for attenuating BMP signaling at synapses. Previous work suggested that Hiw, an E3 ubiquitin ligase and negative regulator of synaptic growth, also acted to limit BMP signaling (McCabe et al., 2004). However, subsequent work demonstrated that pMAD levels are not increased in *hiw* and no effects of Hiw overexpression on BMP signaling have been described (Collins et al., 2006). In addition, *hiw* synapses are extremely expansive, elaborately branched, and contain numerous small boutons, but no satellite boutons (Wan et al., 2000). This phenotype is distinct from that associated with *Tkv^{ACT}* overexpression or other genotypes believed to elevate BMP signaling, including *Dad*, *nwk*, and known endocytic genes – all of which exhibit satellite boutons. Together with the recent finding that Hiw regulates MAPKKK-dependent Fos activity, these observations suggest Hiw and BMP signaling regulate different aspects of synaptic growth.

In their recent study of Spict, Wang et al. (2007) demonstrated the partial colocalization of Spict with early endosomes along with data suggesting that Spict plays a role in BMP receptor trafficking (Wang et al., 2007). For example, Spict overexpression in S2 cells caused Wit to relocalize to early endosomes, suggesting negative regulation of BMP signaling by

sequestering Wit receptor and/or Wit-Gbb signaling complexes. However, studies of Wit trafficking at *spict* NMJs, which are limited by the small size of boutons and the lack of reliable antibodies, did not uncover this trafficking defect but instead revealed increased Wit levels consistent with a role for Spict in the degradation of Wit. Nonetheless, the results from the analysis of Spict support with the idea that endocytic regulation of BMP signaling is required for proper synaptic growth. It will be interesting to determine whether Spict interacts with Nwk or plays a distinct role in the regulation of BMP signaling at synapses.

Overall, our findings support a model in which Nwk constrains synaptic growth by regulating endocytic trafficking of Tkv to attenuate positive retrograde growth signaling. While the simplest model is that Nwk targets Tkv for degradation, we do not observe gross differences in levels of ectopically expressed Tkv-GFP in otherwise wild type, *nwk* and *C155GAL4; UAS-nwk* larvae (unpublished results). A caveat is that without the necessary antibody reagents we are unable to look at endogenous Tkv. Thus, these observations might not accurately reflect normal receptor trafficking but rather the fact that high levels of Tkv can override endogenous regulation. Nonetheless, together with our observation that Nwk colocalizes with Rab11, this finding is consistent with a role for Nwk in BMP receptor recycling. For example, Nwk might attenuate BMP signaling levels by regulating the rate at which vacant Tkv receptors are recycled back to the plasma membrane following activation and internalization. Nwk might also regulate the trafficking of unbound receptors from the plasma membrane. Previous work in vertebrates demonstrates that TGF- β receptors are recycled through a Rab11-dependent mechanism independent of ligand binding, possibly as a means of rapidly and dynamically regulating surface receptor number and, thus, sensitivity to TGF- β (Mitchell et al., 2004). Interestingly, we observe the re-localization of Nwk from a more uniform to a more punctate expression pattern upon overexpression of Tkv (See Figure 7A), consistent with recruitment of Nwk to regulate trafficking of ectopic Tkv. Nwk might also have localized effects within boutons, for example, by restricting sites of BMP signaling through spatial regulation of receptor recycling. It is intriguing to speculate that disruption of spatial constraints on BMP signaling results in ectopic bouton division and, thus, satellite bouton formation. Such a mechanism could provide a critical means for effecting localized changes to existing synapses that underlie neural plasticity. A conceptually similar Rab11-dependent process for the asymmetric activation of Notch signaling in the developing nervous system has recently been described (Emery et al., 2005; Jafar-Nejad et al., 2005). A future challenge will be to further dissect the regulatory mechanisms that control the levels, timing and localization of BMP signaling at synapses. These studies will advance our understanding of the dynamic regulation of synaptic growth and plasticity and likely provide additional general insights into the intricate role of endocytosis in signal transduction.

Experimental Procedures

Fly Stocks

The following fly stocks were used: *nwk*¹, *nwk*² and *UASnwk*^{33D} (Coyle et al., 2004); *dap160*^{EMS}, *dap160*^{A.1} and *UASdap160* (Koh et al., 2004); *mad*¹² (Sekelsky et al., 1995); *gbb*^{D20} (Chen et al., 1998); *elavGAL4* (A. DiAntonio); *UAStkvA*^{B3} (Hoodless et al., 1996); *Dad*²⁷¹⁻⁶⁸ (Tsuneizumi et al., 1997); *UASrab5-GFP* and *UASrab7-GFP* (M. González-Gaitán); and *UAStkv-GFP* (Hsiung et al., 2005). All other stocks were obtained from Bloomington Stock Center.

Immunofluorescence studies

All larvae were obtained from crosses of 10 females and 10 males, to control for crowding, conducted at 25°C. *shi*^{ts1} crosses were kept at room temperature and progeny shifted to 25°C during embryogenesis. Wandering third instar larvae were dissected in ice-cold Ca²⁺-free

saline and fixed for 15 minutes in 4% formaldehyde in PBS. Larvae were incubated in primary antibodies overnight at 4°C or for 4 hours at room temperature and secondary antibodies for 1–2 hours at room temperature then mounted in Vectashield (Vector Laboratories) for microscopic analysis. For comparison of pMAD levels, larvae of all genotypes analyzed were stained in the same dish. *wit* null mutants were analyzed as a control for potential cross-reactivity with Mad. We used the following antibodies: FITC-conjugated anti-HRP at 1:100 (Jackson ImmunoResearch); mouse anti-NC82 (Bruchpilot) at 1:100 (E. Buchner), rat anti-Nwk at 1:1000 (Coyle et al., 2004); rabbit anti-Dap160 and anti-dynamin at 1:100 (Roos and Kelly, 1998); rabbit anti-GFP at 1:500 (Molecular Probes); rabbit anti-PS1 at 1:500 (Persson et al., 1998); rabbit anti-pMAD at 1:100 (Cell Signaling) and mouse anti-Dlg at 1:500 (Developmental Hybridoma Studies Bank). Species-specific Alexa-488 and Alexa-568 (Molecular Probes) were used at 1:200.

Imaging and quantification

Quantification of bouton number was performed at NMJ 4 in segments A2-A4 as described (Coyle et al., 2004). The muscle size of all larvae analyzed was similar. Satellite boutons were defined as extensions of 5 or fewer boutons emanating from the main branch of the nerve terminal. The same control data sets were used for multiple comparisons. We performed the statistical analysis by ANOVA and conducted post hoc tests with the appropriate Bonferroni adjustment for multiple comparisons to ensure an experiment-wise simultaneous significance level of 0.05. While we conducted each comparison at the reduced critical p-value, we report the significance levels at the corresponding experiment-wise levels of less than 0.05, less than 0.01, or less than 0.001, by 1, 2, and 3 stars respectively. Error bars denote SEM. Confocal images were obtained on a Bio-Rad Radiance 2100 MP Rainbow mounted on a Nikon Eclipse TE2000 and processed in NIH ImageJ. Brightness and contrast were adjusted using Adobe Photoshop. Quantification of pMAD intensity was performed on confocal images captured with identical settings using NIH ImageJ software.

Yeast two-hybrid analysis

Yeast two-hybrid experiments were performed using the Clontech Matchmaker system according to their protocols. Drop tests were performed by plating 5µl of serial dilutions of mid-log-phase liquid cultures on appropriate selection media.

GST pulldowns

Nwk, dynamin, Dap160 and Tkv constructs were cloned into the pGEX-6P-3 vector using standard molecular techniques and expressed in bacteria. Fusion proteins were immobilized on glutathione-sepharose beads and incubated with cell extracts prepared from *C155GAL4; UASnwk-RFP* or *C155GAL4; UAStkv-GFP* adult flies. Beads were washed three times in lysis buffer. Bound proteins were eluted and analyzed by western analysis using rabbit anti-dsRed (Clontech) at 1:750 or purified rabbit anti-GFP (Abcam) at 1:1000.

Acknowledgements

We thank Hugo Bellen, Erich Buchner, Aaron DiAntonio, Marcos González-Gaitán, Regis Kelly, Thomas Kornberg, Sean Sweeney, Peter ten Dijke, Kristi Wharton, the Bloomington Stock Center and the Developmental Studies Hybridoma Bank for generously providing fly stocks and antibodies. We are grateful to members of the Ganetzky lab and Avital Rodal for helpful discussions and to Heather Broihier, Tim Fergestad and Daniel Miller for critical comments on the manuscript. We also thank Katherine Hannon and Veena Rao for the many dissections they performed during the course of this work and Noah Rozich for assistance with biochemical experiments. This research was supported by an NIH grant (NS-15390) to B.G. and a fellowship from The Jane Coffin Childs Memorial Fund for Medical Research to K.M.G.

References

- Aberle H, Haghighi AP, Fetter RD, McCabe BD, Magalhaes TR, Goodman CS. wishful thinking encodes a BMP type II receptor that regulates synaptic growth in *Drosophila*. *Neuron* 2002;33:545–558. [PubMed: 11856529]
- Allan DW, St Pierre SE, Miguel-Aliaga I, Thor S. Specification of neuropeptide cell identity by the integration of retrograde BMP signaling and a combinatorial transcription factor code. *Cell* 2003;113:73–86. [PubMed: 12679036]
- Bokel C, Schwabedissen A, Entchev E, Renaud O, Gonzalez-Gaitan M. Sara endosomes and the maintenance of Dpp signaling levels across mitosis. *Science (New York, N.Y)* 2006;314:1135–1139.
- Budnik V, Zhong Y, Wu CF. Morphological plasticity of motor axons in *Drosophila* mutants with altered excitability. *J Neurosci* 1990;10:3754–3768. [PubMed: 1700086]
- Chen Y, Riese MJ, Killinger MA, Hoffmann FM. A genetic screen for modifiers of *Drosophila* decapentaplegic signaling identifies mutations in *punt*, *Mothers against dpp* and the BMP-7 homologue, *60A*. *Development (Cambridge, England)* 1998;125:1759–1768.
- Collins CA, DiAntonio A. Synaptic development: insights from *Drosophila*. *Current opinion in neurobiology* 2007;17:35–42. [PubMed: 17229568]
- Collins CA, Waikar YP, Johnson SL, DiAntonio A. Highwire restrains synaptic growth by attenuating a MAP kinase signal. *Neuron* 2006;51:57–69. [PubMed: 16815332]
- Conner SD, Schmid SL. Regulated portals of entry into the cell. *Nature* 2003;422:37–44. [PubMed: 12621426]
- Coyle IP, Koh YH, Lee WC, Slind J, Fergestad T, Littleton JT, Ganetzky B. Nervous wreck, an SH3 adaptor protein that interacts with Wsp, regulates synaptic growth in *Drosophila*. *Neuron* 2004;41:521–534. [PubMed: 14980202]
- Di Fiore PP, De Camilli P. Endocytosis and signaling. an inseparable partnership. *Cell* 2001;106:1–4. [PubMed: 11461694]
- Dickman DK, Lu Z, Meinertzhagen IA, Schwarz TL. Altered synaptic development and active zone spacing in endocytosis mutants. *Curr Biol* 2006;16:591–598. [PubMed: 16546084]
- Dillon C, Goda Y. The actin cytoskeleton: integrating form and function at the synapse. *Annual review of neuroscience* 2005;28:25–55.
- Dudu V, Bittig T, Entchev E, Kicheva A, Julicher F, Gonzalez-Gaitan M. Postsynaptic mad signaling at the *Drosophila* neuromuscular junction. *Curr Biol* 2006;16:625–635. [PubMed: 16581507]
- Emery G, Hutterer A, Berdnik D, Mayer B, Wirtz-Peitz F, Gaitan MG, Knoblich JA. Asymmetric Rab 11 endosomes regulate delta recycling and specify cell fate in the *Drosophila* nervous system. *Cell* 2005;122:763–773. [PubMed: 16137758]
- Engqvist-Goldstein AE, Drubin DG. Actin assembly and endocytosis: from yeast to mammals. *Annual review of cell and developmental biology* 2003;19:287–332.
- Estes PS, Roos J, van der Blik A, Kelly RB, Krishnan KS, Ramaswami M. Traffic of dynamin within individual *Drosophila* synaptic boutons relative to compartment-specific markers. *J Neurosci* 1996;16:5443–5456. [PubMed: 8757257]
- Haghighi AP, McCabe BD, Fetter RD, Palmer JE, Hom S, Goodman CS. Retrograde control of synaptic transmission by postsynaptic CaMKII at the *Drosophila* neuromuscular junction. *Neuron* 2003;39:255–267. [PubMed: 12873383]
- Hayes S, Chawla A, Corvera S. TGF beta receptor internalization into EEA1-enriched early endosomes: role in signaling to Smad2. *The Journal of cell biology* 2002;158:1239–1249. [PubMed: 12356868]
- Hoang B, Chiba A. Single-cell analysis of *Drosophila* larval neuromuscular synapses. *Developmental biology* 2001;229:55–70. [PubMed: 11133154]
- Hoodless PA, Haerry T, Abdollah S, Stapleton M, O'Connor MB, Attisano L, Wrana JL. MADR1, a MAD-related protein that functions in BMP2 signaling pathways. *Cell* 1996;85:489–500. [PubMed: 8653785]
- Hsiung F, Ramirez-Weber FA, Iwaki DD, Kornberg TB. Dependence of *Drosophila* wing imaginal disc cytonemes on Decapentaplegic. *Nature* 2005;437:560–563. [PubMed: 16177792]

- Hussain NK, Jenna S, Glogauer M, Quinn CC, Wasiak S, Guipponi M, Antonarakis SE, Kay BK, Stossel TP, Lamarche-Vane N, McPherson PS. Endocytic protein intersectin-1 regulates actin assembly via Cdc42 and N-WASP. *Nature cell biology* 2001;3:927–932.
- Itoh T, De Camilli P. BAR, F-BAR (EFC) and ENTH/ANTH domains in the regulation of membrane-cytosol interfaces and membrane curvature. *Biochimica et biophysica acta* 2006;1761:897–912. [PubMed: 16938488]
- Itoh T, Erdmann KS, Roux A, Habermann B, Werner H, De Camilli P. Dynamin and the actin cytoskeleton cooperatively regulate plasma membrane invagination by BAR and F-BAR proteins. *Developmental cell* 2005;9:791–804. [PubMed: 16326391]
- Jafar-Nejad H, Andrews HK, Acar M, Bayat V, Wirtz-Peitz F, Mehta SQ, Knoblich JA, Bellen HJ. Sec15, a component of the exocyst, promotes notch signaling during the asymmetric division of *Drosophila* sensory organ precursors. *Developmental cell* 2005;9:351–363. [PubMed: 16137928]
- Keshishian H, Kim YS. Orchestrating development and function: retrograde BMP signaling in the *Drosophila* nervous system. *Trends in neurosciences* 2004;27:143–147. [PubMed: 15036879]
- Khodosh R, Augsburger A, Schwarz TL, Garrity PA. Bchs, a BEACH domain protein, antagonizes Rab11 in synapse morphogenesis and other developmental events. *Development (Cambridge, England)* 2006;133:4655–4665.
- Kim Y, Chang S. Ever-expanding network of dynamin-interacting proteins. *Molecular neurobiology* 2006;34:129–136. [PubMed: 17220534]
- Koh TW, Verstreken P, Bellen HJ. Dap160/intersectin acts as a stabilizing scaffold required for synaptic development and vesicle endocytosis. *Neuron* 2004;43:193–205. [PubMed: 15260956]
- Marie B, Sweeney ST, Poskanzer KE, Roos J, Kelly RB, Davis GW. Dap160/intersectin scaffolds the periaxonal zone to achieve high-fidelity endocytosis and normal synaptic growth. *Neuron* 2004;43:207–219. [PubMed: 15260957]
- Marques G, Bao H, Haerry TE, Shimell MJ, Duchek P, Zhang B, O'Connor MB. The *Drosophila* BMP type II receptor Wishful Thinking regulates neuromuscular synapse morphology and function. *Neuron* 2002;33:529–543. [PubMed: 11856528]
- Marrus SB, DiAntonio A. Preferential localization of glutamate receptors opposite sites of high presynaptic release. *Curr Biol* 2004;14:924–931. [PubMed: 15182665]
- McCabe BD, Hom S, Aberle H, Fetter RD, Marques G, Haerry TE, Wan H, O'Connor MB, Goodman CS, Haghghi AP. Highwire regulates presynaptic BMP signaling essential for synaptic growth. *Neuron* 2004;41:891–905. [PubMed: 15046722]
- McCabe BD, Marques G, Haghghi AP, Fetter RD, Crotty ML, Haerry TE, Goodman CS, O'Connor MB. The BMP homolog Gbb provides a retrograde signal that regulates synaptic growth at the *Drosophila* neuromuscular junction. *Neuron* 2003;39:241–254. [PubMed: 12873382]
- Mitchell H, Choudhury A, Pagano RE, Leof EB. Ligand-dependent and -independent transforming growth factor-beta receptor recycling regulated by clathrin-mediated endocytosis and Rab11. *Molecular biology of the cell* 2004;15:4166–4178. [PubMed: 15229286]
- Miyazono K, Kusanagi K, Inoue H. Divergence and convergence of TGF-beta/BMP signaling. *Journal of cellular physiology* 2001;187:265–276. [PubMed: 11319750]
- Nakayama H, Kazama H, Nose A, Morimoto-Tanifuji T. Activity-dependent regulation of synaptic size in *Drosophila* neuromuscular junctions. *Journal of neurobiology* 2006;66:929–939. [PubMed: 16758490]
- Packard M, Koo ES, Gorczyca M, Sharpe J, Cumberledge S, Budnik V. The *Drosophila* Wnt, wingless, provides an essential signal for pre- and postsynaptic differentiation. *Cell* 2002;111:319–330. [PubMed: 12419243]
- Persson U, Izumi H, Souchelnytskyi S, Itoh S, Grimsby S, Engstrom U, Heldin CH, Funahashi K, ten Dijke P. The L45 loop in type I receptors for TGF-beta family members is a critical determinant in specifying Smad isoform activation. *FEBS letters* 1998;434:83–87. [PubMed: 9738456]
- Pielage J, Fetter RD, Davis GW. A postsynaptic spectrin scaffold defines active zone size, spacing, and efficacy at the *Drosophila* neuromuscular junction. *The Journal of cell biology* 2006;175:491–503. [PubMed: 17088429]

- Rawson JM, Lee M, Kennedy EL, Selleck SB. Drosophila neuromuscular synapse assembly and function require the TGF-beta type I receptor saxophone and the transcription factor Mad. *Journal of neurobiology* 2003;55:134–150. [PubMed: 12672013]
- Roos J, Kelly RB. Dap160, a neural-specific Eps15 homology and multiple SH3 domain-containing protein that interacts with Drosophila dynamin. *The Journal of biological chemistry* 1998;273:19108–19119. [PubMed: 9668096]
- Roos J, Kelly RB. The endocytic machinery in nerve terminals surrounds sites of exocytosis. *Curr Biol* 1999;9:1411–1414. [PubMed: 10607569]
- Saitoe M, Schwarz TL, Umbach JA, Gundersen CB, Kidokoro Y. Absence of junctional glutamate receptor clusters in Drosophila mutants lacking spontaneous transmitter release. *Science (New York, N.Y)* 2001;293:514–517.
- Schenck A, Qurashi A, Carrera P, Bardoni B, Diebold C, Schejter E, Mandel JL, Giangrande A. WAVE/SCAR, a multifunctional complex coordinating different aspects of neuronal connectivity. *Developmental biology* 2004;274:260–270. [PubMed: 15385157]
- Sekelsky JJ, Newfeld SJ, Raftery LA, Chartoff EH, Gelbart WM. Genetic characterization and cloning of mothers against dpp, a gene required for decapentaplegic function in Drosophila melanogaster. *Genetics* 1995;139:1347–1358. [PubMed: 7768443]
- Sigrist SJ, Reiff DF, Thiel PR, Steinert JR, Schuster CM. Experience-dependent strengthening of Drosophila neuromuscular junctions. *J Neurosci* 2003;23:6546–6556. [PubMed: 12878696]
- Sigrist SJ, Thiel PR, Reiff DF, Schuster CM. The postsynaptic glutamate receptor subunit DGluR-IIA mediates long-term plasticity in Drosophila. *J Neurosci* 2002;22:7362–7372. [PubMed: 12196557]
- Smythe E, Ayscough KR. Actin regulation in endocytosis. *Journal of cell science* 2006;119:4589–4598. [PubMed: 17093263]
- Sweeney ST, Davis GW. Unrestricted synaptic growth in spinster-a late endosomal protein implicated in TGF-beta-mediated synaptic growth regulation. *Neuron* 2002;36:403–416. [PubMed: 12408844]
- Takenawa T, Suetsugu S. The WASP-WAVE protein network: connecting the membrane to the cytoskeleton. *Nature reviews* 2007;8:37–48.
- Tsuneizumi K, Nakayama T, Kamoshida Y, Kornberg TB, Christian JL, Tabata T. Daughters against dpp modulates dpp organizing activity in Drosophila wing development. *Nature* 1997;389:627–631. [PubMed: 9335506]
- Wan HI, DiAntonio A, Fetter RD, Bergstrom K, Strauss R, Goodman CS. Highwire regulates synaptic growth in Drosophila. *Neuron* 2000;26:313–329. [PubMed: 10839352]
- Wang X, Shaw WR, Tsang HT, Reid E, O'Kane CJ. Drosophila spichthyn inhibits BMP signaling and regulates synaptic growth and axonal microtubules. *Nature neuroscience* 2007;10:177–185.
- Zamanian JL, Kelly RB. Intersectin 1L guanine nucleotide exchange activity is regulated by adjacent src homology 3 domains that are also involved in endocytosis. *Molecular biology of the cell* 2003;14:1624–1637. [PubMed: 12686614]

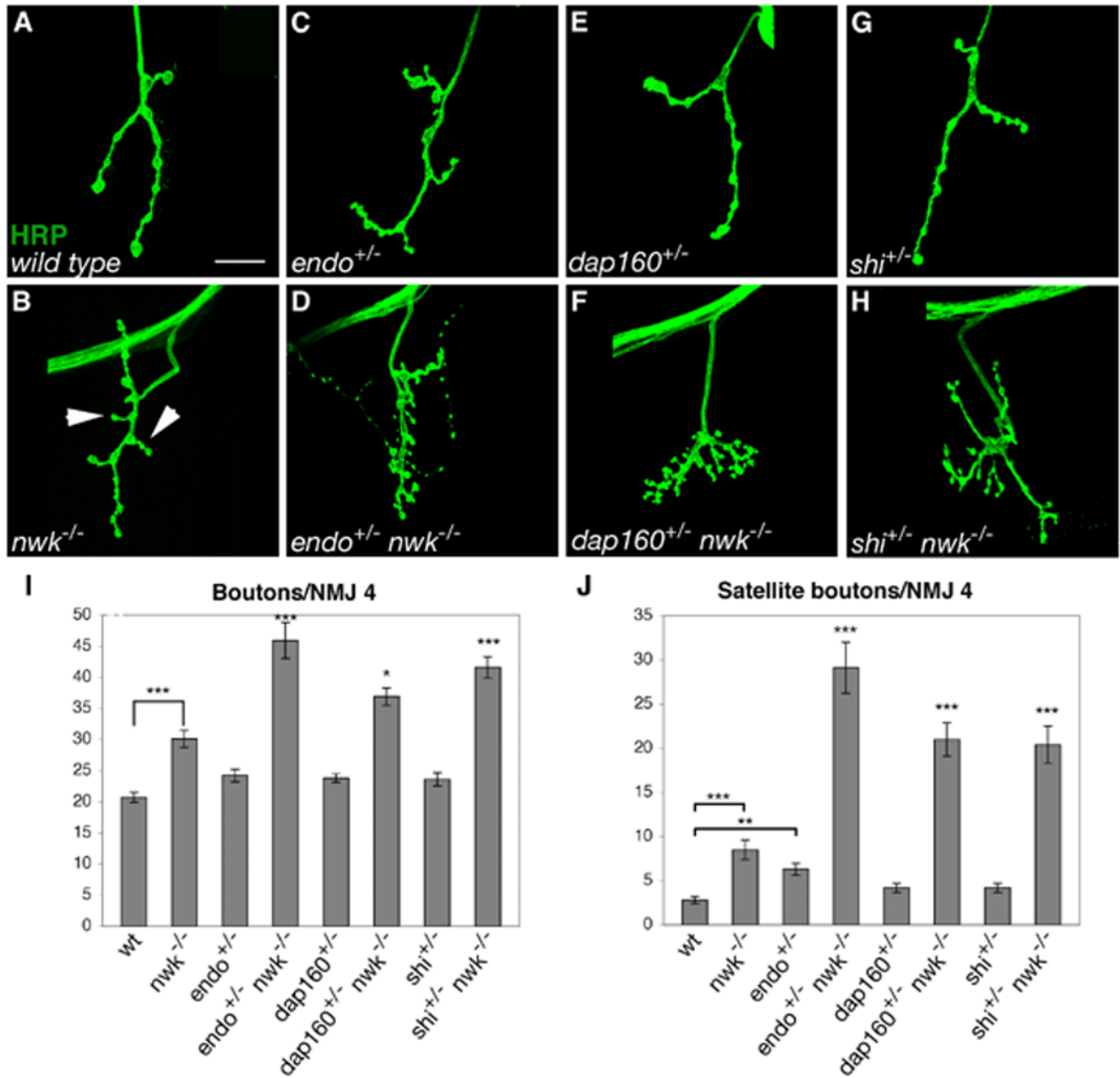


Figure 1. Synaptic overgrowth in *nwk* is dominantly enhanced by endocytic mutations

(A–H) Confocal images of NMJ 4 labeled with FITC-conjugated anti-HRP. (A) Wild-type NMJs are relatively unbranched and contain few satellite boutons. (B) *nwk* NMJs are more branched than wild type and have increased numbers of total boutons and satellite boutons. (C–D) Loss of one copy of *endo* has no effect on total and a small effect on satellite bouton formation in a wild-type background (C), but results in a large increase in both parameters in a *nwk* background (D). (E–F) Loss of one copy of *dap160* does not affect bouton number or satellite bouton formation in a wild-type background (E), but leads to a significant increase in total and satellite bouton number in *nwk* mutants (F). (G–H) At the semi-restrictive temperature of 25°C, heterozygosity for *shi* does not affect total or satellite bouton number at wild-type NMJs (G), but in a *nwk* background, total bouton number and satellite bouton formation are significantly increased (H). (I–J) Quantification of total (I) and satellite (J) bouton number at NMJ 4 in wild type, *nwk*^{1/2}, *endo*^{2730/+}, *endo*²⁷³⁰ *nwk*^{2/+} *nwk*¹, *dap160*^{Δ1/+}, *dap160*^{Δ1/+}; *nwk*^{1/2}, *shi*^{ts1/+}, and *shi*^{ts1/+}; *nwk*^{1/2} backgrounds. * p < 0.05, ** p < 0.01, *** p < 0.001. P-

values above individual bars refer to comparisons between *nwk* and the indicated genotype. Arrows in B point to examples of satellite boutons. Scale bar equals 20 μ M.

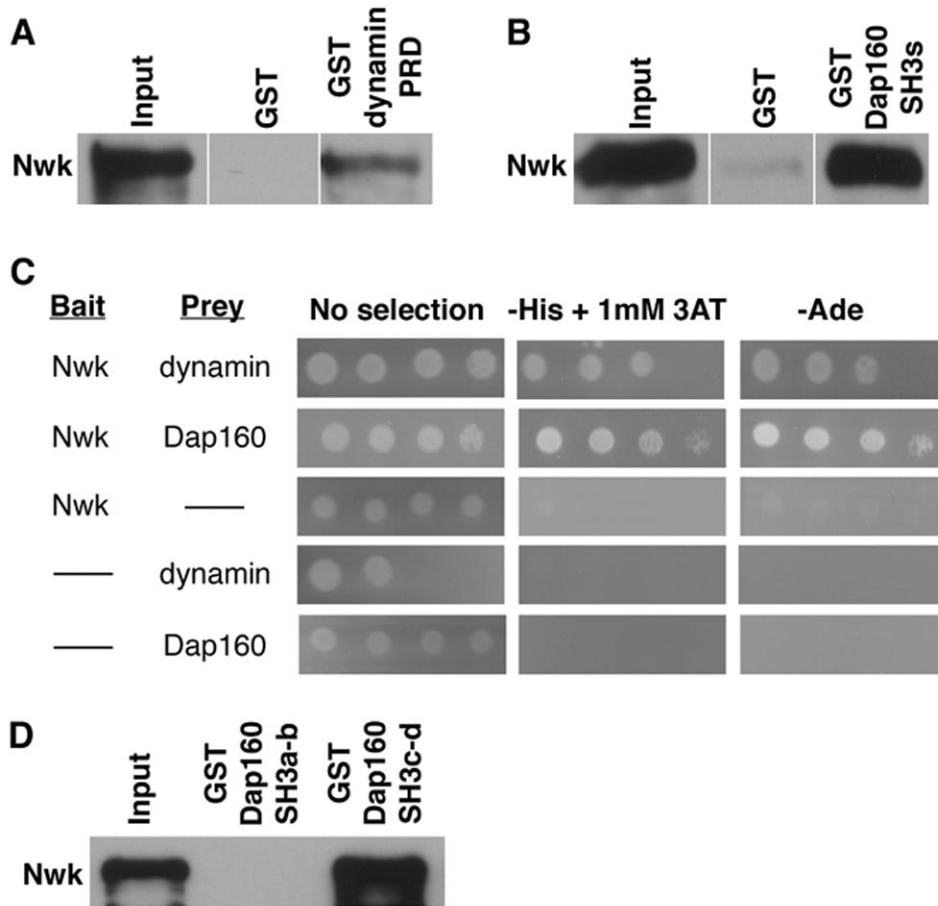


Figure 2. Nwk physically interacts with dynamin and Dap160

(A) A dynamin-PRD-GST-fusion protein precipitates Nwk-RFP from *C155GAL4; UASnwk-RFP* fly lysates with high affinity, while GST alone does not. (B) GST-Dap160SH3a-d precipitates Nwk-RFP from cellular lysates. (C) Yeast two-hybrid interactions demonstrate a direct association between full-length Nwk and the proline-rich domain (PRD) of dynamin and between Nwk and the SH3 domains of Dap160. Full-length Nwk is fused to the GAL4 DNA-binding domain (prey) and the dynamin PRD and Dap160 SH3 domains are fused to the GAL4 activation domain (bait). After 3 days at 30°C, yeast transformed with either bait or prey alone grow only in the absence of selection, whereas yeast coexpressing both bait and prey fusion proteins exhibit growth on SD medium lacking either histidine or adenine indicating that transcription of reporter genes has been activated. 3AT inhibits His3p activity and increases the stringency of selection. (D) Dap160-SH3c-d, but not Dap160-SH3a-b, GST-fusion protein precipitates Nwk-RFP from cell lysates. A, B and D are probed with rabbit anti-dsRed; input lanes contain lysate equal to 1/10 of the amount used for the pull-down assays.

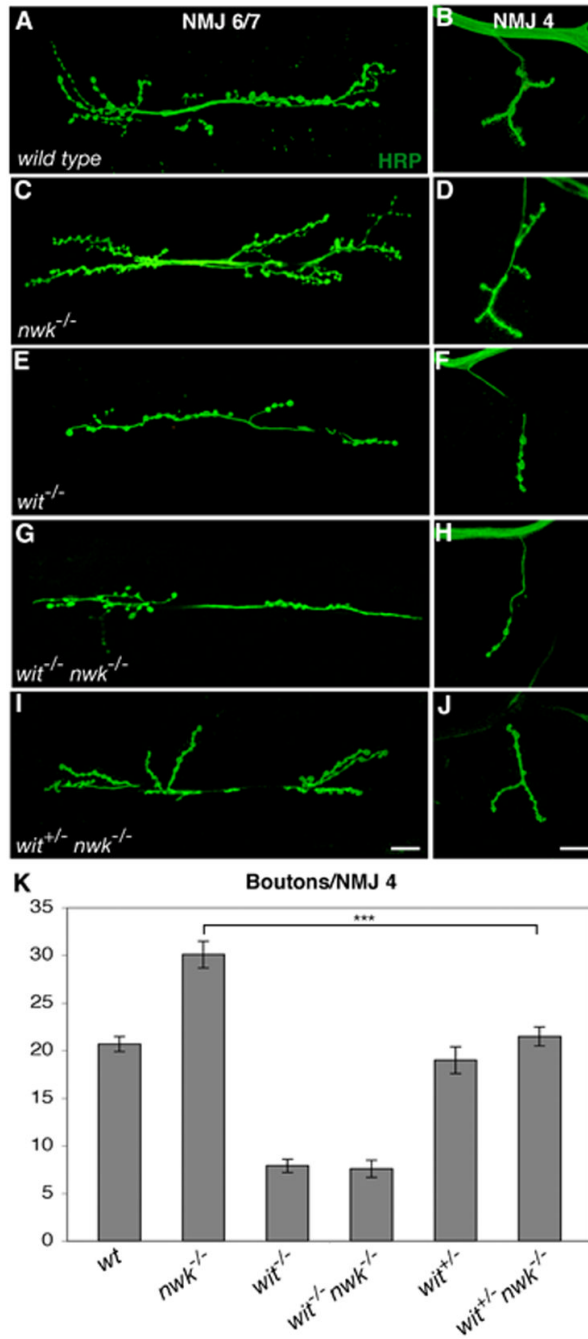


Figure 3. Synaptic overgrowth in *nwk* is sensitive to BMP signaling levels

(A–J) Confocal images of NMJ 6/7 (A, C, E, G and I) and NMJ 4 (B, D, F, H and J) labeled with FITC-conjugated anti-HRP. (A, B) wild type. (C, D) *nwk*^{1/2} mutants exhibit synaptic overgrowth. (E, F) *wit*^{A12/B11} mutants have dramatically undergrown synapses. (G, H) *wit*^{A12} *nwk*² double mutants exhibit synaptic undergrowth that is essentially identical to that observed in *wit* single mutants. (I, J) Loss of one copy of *wit* dominantly suppresses synaptic overgrowth of *nwk* (*wit*^{A12/+} *nwk*^{1/2}). (K) Quantification of bouton number at NMJ 4 in wild type, *nwk*^{1/2}, *wit*^{A12/B11}, *wit*^{A12} *nwk*², *wit*^{A12/+} and *wit*^{A12} *nwk*^{2/+} *nwk*¹ backgrounds. *** *p* < 0.001. Scale bars equal 20 μM.

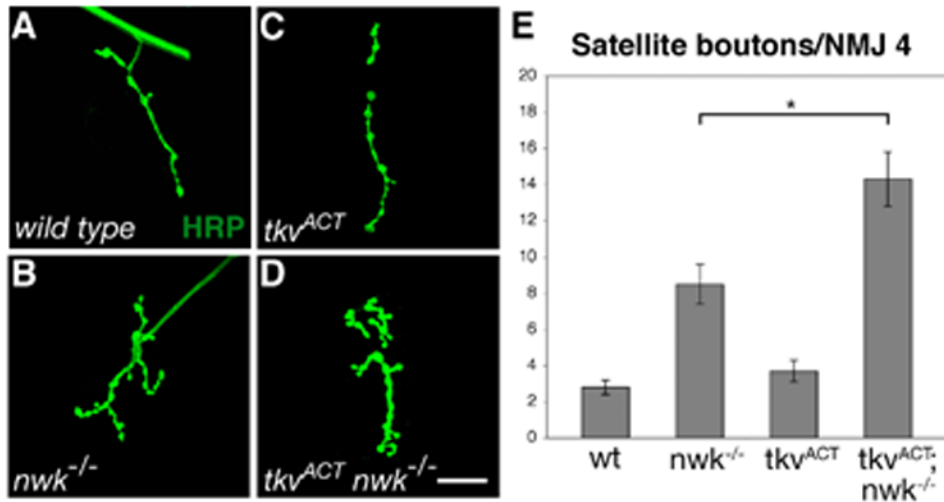


Figure 4. Nwk constrains BMP-induced synaptic overgrowth

(A–D) Confocal images of NMJ 4 labeled with FITC-conjugated anti-HRP. (A) wild type. (B) *nwk*^{1/2}. (C) Neuronal expression of *Tkv*^{ACT} in a wild-type background does not result in an increase in satellite bouton number. (D) *Tkv*^{ACT} expression in the absence of *nwk* results in an increase in satellite boutons over that resulting from loss of *nwk* alone. (E) Quantification of satellite bouton number at NMJ 4 in wild type, *nwk*^{1/2}, *elavGAL4/UAStkv*^{ACT} and *elavGAL4 nwk*^{2/UAStkv^{ACT} *nwk*² backgrounds. * $p < 0.05$. Scale bar equals 20 μ M.}

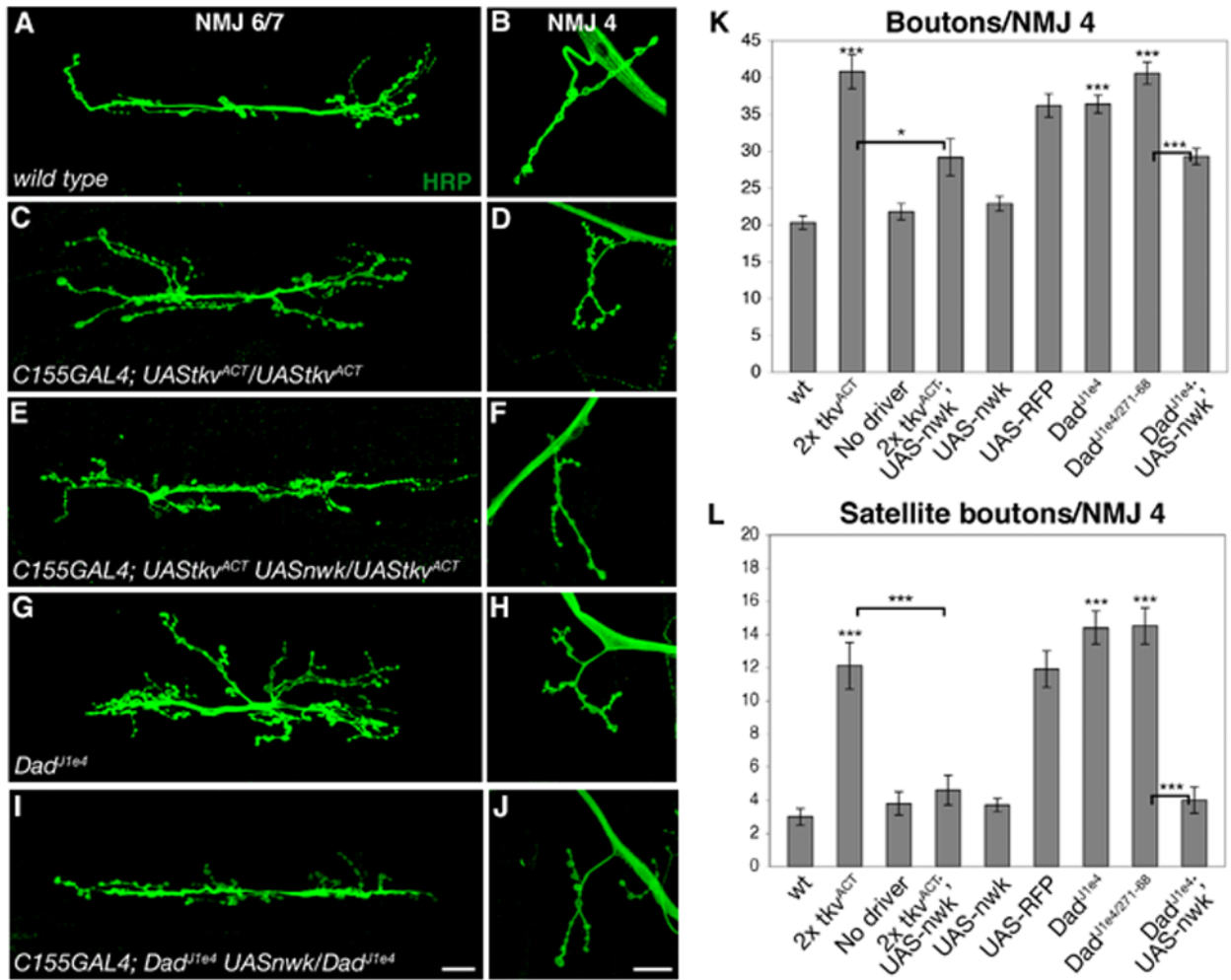


Figure 5. BMP-induced synaptic overgrowth is suppressed by neuronal overexpression of Nwk (A–J) Confocal images of NMJ 6/7 (A, C, E, G and I) and NMJ 4 (B, D, F, H and J) labeled with FITC-conjugated anti-HRP. (A, B) wild type. (C, D) *C155GAL4; UAStkv^{ACT}/UAStkv^{ACT}* synapses display an increase in bouton number and satellite bouton formation demonstrating that sufficiently high levels of BMP signaling can induce synaptic overgrowth. (E, F) Neuronal overexpression of Nwk suppresses *Tkv^{ACT}*-induced synaptic overgrowth. (G, H) Increased bouton number and satellite bouton formation are observed in *Dad^{J1e4}* mutants, demonstrating that loss of negative regulation of BMP signaling results in synaptic overgrowth. (I, J) Synaptic overgrowth in *Dad^{J1e4}* is suppressed by neuronal overexpression of Nwk. (K, L) Quantification of total (K) and satellite (L) bouton number at NMJ 4 in wild type, *C155GAL4; UAStkv^{ACT}/UAStkv^{ACT}*, *UAStkv^{ACT}/UAStkv^{ACT}*, *C155GAL4; UAStkv^{ACT} UASnwk/UAStkv^{ACT}*, *C155GAL4; UASnwk/+*, *C155GAL4; UAStkv^{ACT}/UASmyrRFP/UAStkv^{ACT}*, *Dad^{J1e4}*, *Dad^{J1e4}/Dad²⁷¹⁻⁶⁸* and *C155GAL4; Dad^{J1e4} UASnwk/Dad^{J1e4}* backgrounds. * $p < 0.05$, *** $p < 0.001$. P-values above individual bars refer to comparisons between wild type and the indicated genotype. Scale bars equal 20 μ M.

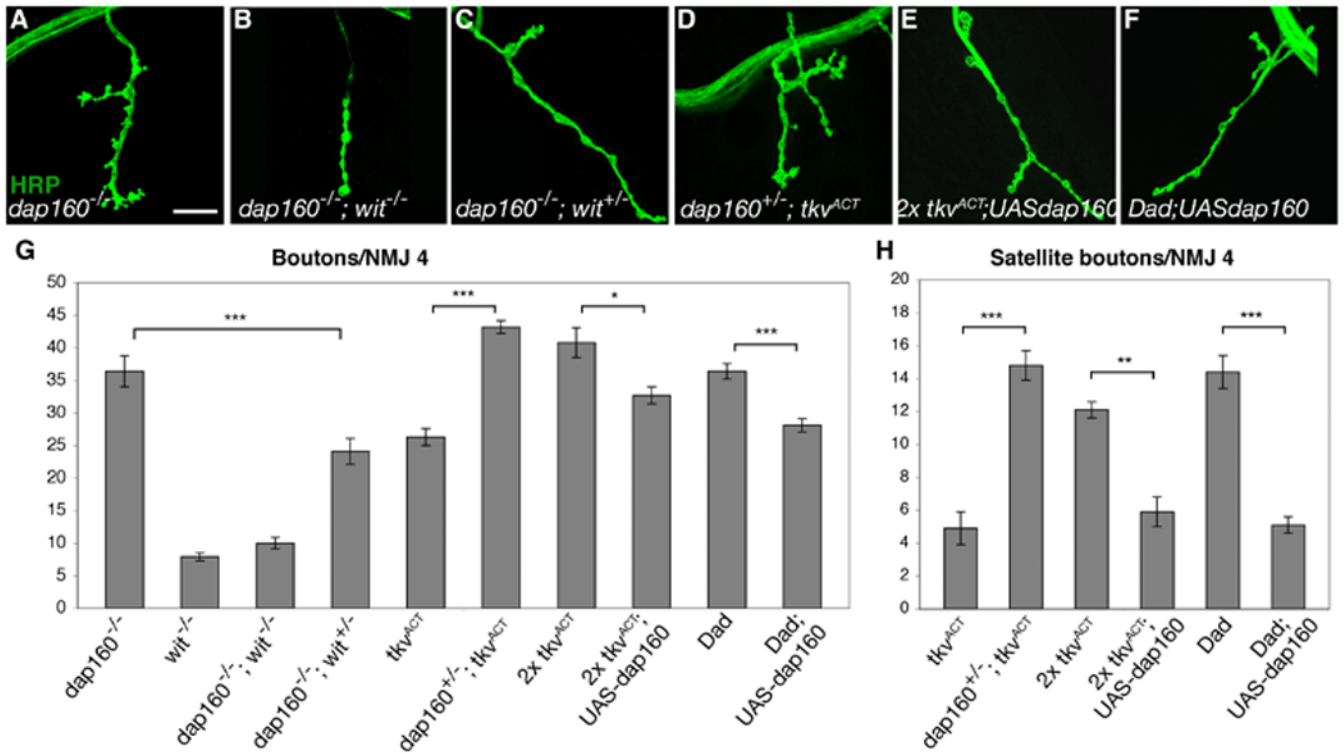


Figure 6. *dap160* interacts with BMP signaling pathway components

(A–F) Confocal images of NMJ 4 labeled with FITC-conjugated anti-HRP. (A) Synaptic overgrowth in *dap160^{Δ1/EMS}*. (B) *dap160^{Δ1}; wit^{A12/B11}* double mutants exhibit the *wit* synaptic undergrowth phenotype. (C) Loss of one copy of *wit* suppresses synaptic overgrowth in *dap160* mutants. (D) Reducing the dose of *dap160* by 50% facilitates *Tkv^{ACT}*-induced synaptic overgrowth. (E–F) Neuronal overexpression of Dap160 suppresses synaptic overgrowth in neurons expressing two copies of *Tkv^{ACT}* (E) and lacking *Dad* (F). (G) Quantification of total bouton number at NMJ 4 in *dap160^{Δ1/EMS}*, *wit^{A12/B11}*, *dap160^{Δ1/Δ1}; wit^{A12/B11}*, *dap160^{Δ1/Δ1}; wit^{A12/+}*, *C155GAL4; UAStkv^{ACT/+}*, *C155GAL4; dap160^{Δ1/+}; UAStkv^{ACT/+}*, *C155GAL4; UAStkv^{ACT/UAStkv^{ACT}}*, *C155GAL4; UAStkv^{ACT} UASdap160/UAStkv^{ACT}*, *Dad^{J1e4/J1e4}* and *C155GAL4; Dad^{J1e4} UASdap160/Dad^{J1e4}* backgrounds. (H) Quantification of satellite boutons at NMJ 4 in *C155GAL4; UAStkv^{ACT/+}*, *C155GAL4; dap160^{Δ1/+}; UAStkv^{ACT/+}*, *C155GAL4; UAStkv^{ACT/UAStkv^{ACT}}*, *C155GAL4; UAStkv^{ACT} UASdap160/UAStkv^{ACT}*, *Dad^{J1e4/J1e4}* and *C155GAL4; Dad^{J1e4} UASdap160/Dad^{J1e4}*. * $p < 0.05$, ** $p < 0.01$, *** $p < 0.001$. Scale bar equals 20 μ M.

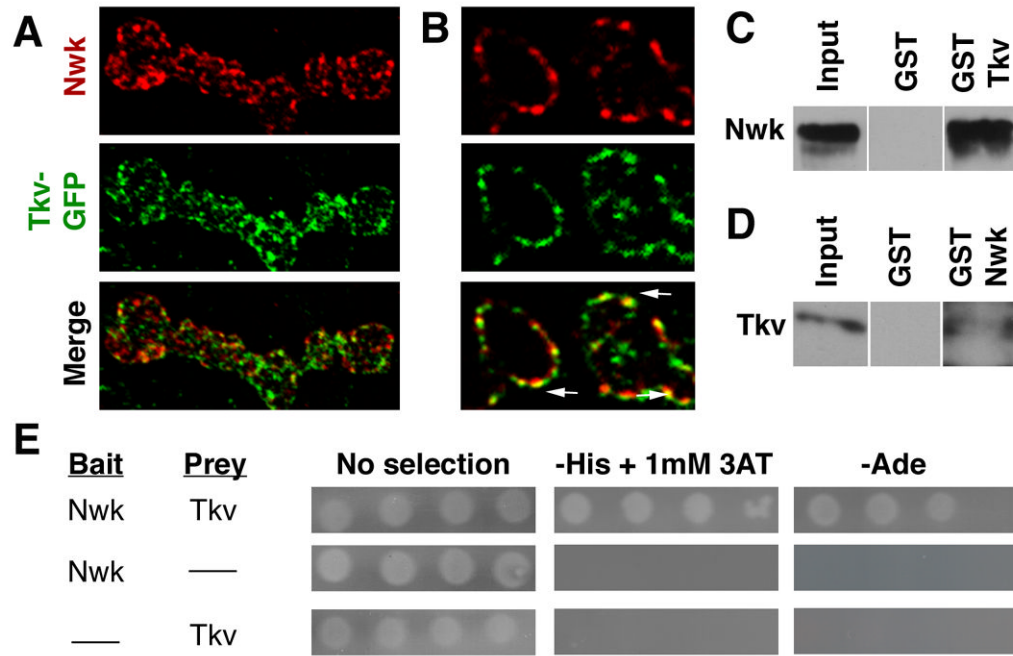


Figure 7. Nwk physically associates with Tkv

(A) Z-series projection of *C155GAL4; UAStkv-GFP* boutons co-labeled with antibodies to Nwk. Note that while both proteins exhibit periaxonal localization, both also localize to discrete puncta. (B) Thin ($0.1\mu\text{m}$) optical cross section of *C155GAL4; UAStkv-GFP* boutons co-labeled with antibodies to Nwk. Arrows indicate several examples of colocalization of Nwk and Tkv-GFP to membrane-associated puncta. (C) GST-Tkv-IC precipitates Nwk-RFP from *C155GAL4; UASnwk-RFP* fly lysates with high affinity. Nwk-RFP is detected with rabbit anti-Red. We obtained similar results in analogous experiments using lysate from wild-type flies expressing only endogenous Nwk, excluding potential artifacts due to overexpression of Nwk or the RFP tag (data not shown). (D) GST-Nwk precipitates full-length tagged-Tkv from *C155GAL4; UAStkv-GFP* lysates as detected by rabbit anti-GFP. Input lanes in C and D contain lysate equal to approximately 1/10 of the amount used for the pull-down assays. (E) Yeast two-hybrid interactions demonstrate direct binding of full-length Nwk (prey) and Tkv-IC (bait). After 3 days at 30°C , only yeast coexpressing both bait and prey fusion proteins exhibit growth on SD medium lacking either histidine or adenine.

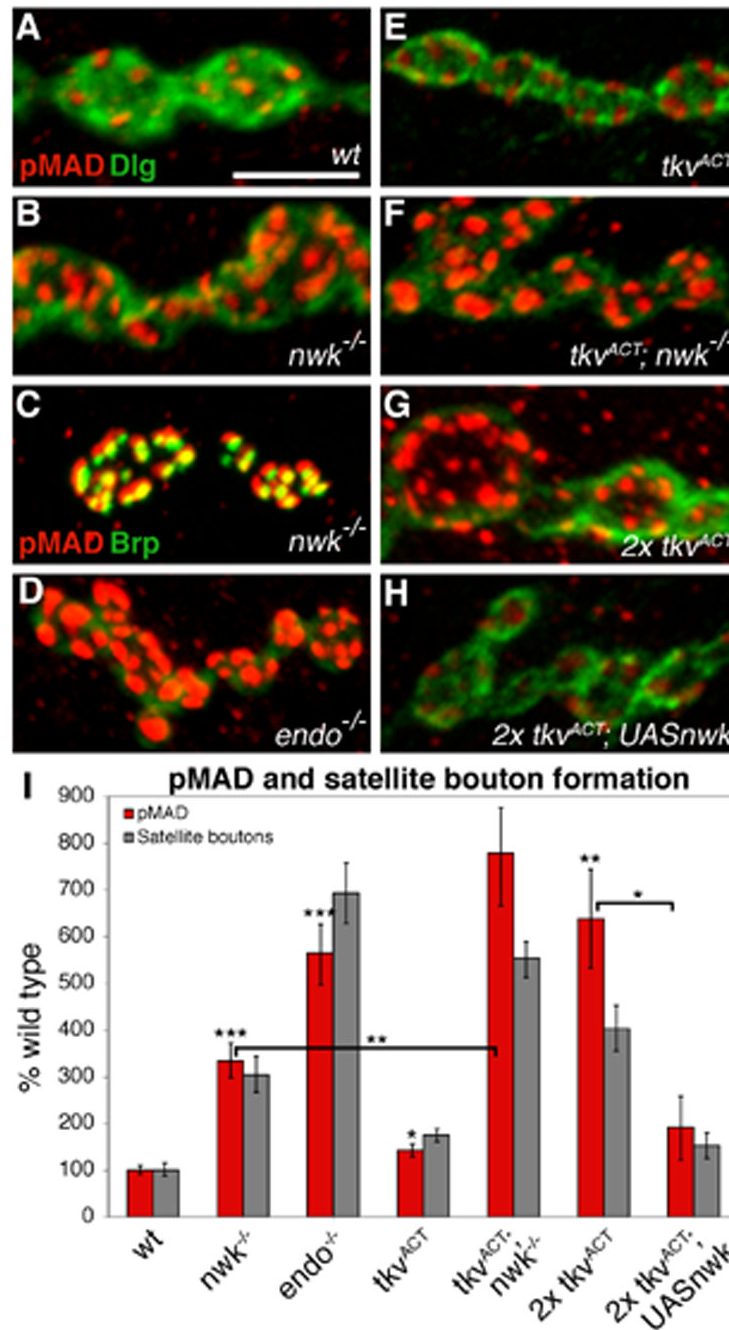


Figure 8. pMAD levels vary with Nwk expression and correlate with satellite bouton formation (A–B, D–H) High magnification images of boutons labeled with rabbit anti-pMAD (red) and mouse anti-Dlg (green) in (A) wild type, (B) *nwk*^{1/2}, (D) *endo*²⁷³⁰, (E) *C155GAL4; UAStkv^{ACT}/+*, (F) *C155GAL4; nwk¹/UAStkv^{ACT} nwk²*, (G) *C155GAL4; UAStkv^{ACT}/UAStkv^{ACT}*, and (H) *C155GAL4; UAStkv^{ACT} UASnwk/UAStkv^{ACT}* boutons. pMAD levels are increased in endocytic mutants (B,D) and in response to ectopic BMP signaling (E,G). While loss of Nwk enhances (F), overexpression of Nwk suppresses (H) BMP-induced pMAD expression. (C) A high magnification image of *nwk* boutons labeled with rabbit anti-pMAD (red) and mouse anti-NC82 (green), which labels the active zone protein Bruchpilot (Brp), shows localization of pMAD to presynaptic terminals. Note that in (B), pMAD does not

colocalize with the postsynaptic marker Dlg. (I) Quantification of pMAD levels normalized for control (Discs large) intensity (red bars). pMAD levels show a strong correspondence to satellite bouton number (grey bars). * $p < 0.05$, ** $p < 0.01$, *** $p < 0.001$. P-values above individual bars refer to comparisons between wild type and the indicated genotype. Scale bar equals 5 μM .